The expression of PKM1 and PKM2 in developing, benign, and cancerous prostatic tissues

Lin Li[1, 2], Siyuan Cheng[1,2], Yunshin Yeh[3], Yingli Shi[1,2], Nikayla Henderson[1], David Price[4], Xin Gu[5], Xiuping Yu[1,2,4]

1. Department of Biochemistry and Molecular biology, LSU Health Shreveport, Shreveport, LA
2. Feist-Weiller Cancer Center, LSU Health Shreveport, Shreveport, LA
3. Pathology & Laboratory Medicine Service, Overton Brooks VA Medical Centesr, Shreveport, LA, USA
4. Department of Urology, LSU Health Shreveport, Shreveport, LA
5. Department of Pathology, LSU Health Shreveport, Shreveport, LA

Correspondence to X. Yu, xiuping.yu@lsuhs.edu

Abstract: Neuroendocrine prostate cancer (NEPCa) is the most aggressive type of prostate cancer. However, energy metabolism, one of the cancer hallmarks, in NEPC had not been well studied yet. Pyruvate kinase M (PKM), which catalyzes the final step of glycolysis, has two main splicing isoforms, PKM1 and PKM2. PKM2 is known to be upregulated in various cancers, including prostate adenocarcinoma (AdPCa). In this study, we used immunohistochemistry, immunofluorescence, and bioinformatic analysis to study the expression of PKM1 and PKM2 in mouse and human prostatic tissues, including developing, benign and cancerous prostate. We found that PKM2 was the predominant isoform expressed throughout the prostate development and PCa progression, with slightly reduced expression in some NEPCa cases. PKM1 was mostly expressed in stroma cells but low levels PKM1 was also detected in prostate basal epithelial cells. PKM1 was also expressed in a subset of NEPCa specimens. Additionally, we identified ten PKM isoforms that express exon 9 (PKM1-like) or exon 10 (PKM2-like). Some of these isoforms showed notable expression levels in PCa cell lines. These findings lay the groundwork for understanding PKMs' role in PCa carcinogenesis and NEPCa progression. The distinct expression patterns of PKM isoforms in different prostate cancer subtypes may offer insights into potential therapeutic strategies and precision medicine.

Key words: PKM1, PKM2, neuroendocrine, prostate cancer, UGS.

1. Introduction

The prostate is a male reproductive accessory gland. It comprises multiple cell types including luminal epithelial, basal epithelial and stromal cells[1]. Prostate cancer (PCa) primarily originates from luminal epithelial cells, thus majority of PCa cases are prostate adenocarcinoma (AdPCa)[2]. AdPCa cells inherited prostate luminal epithelial differentiation markers, such as AR, HOXB13, NKX3.1, and FOXA[3,4]. Androgen deprivation therapy (ADT) is the first-line therapy for advanced AdPCa[5]. However, ADT eventually fails and PCa relapses and progress into more aggressive castrate-resistant prostate cancer[6-8]. With heightened androgen blockade, more aggressive neuroendocrine prostate cancer (NEPCa) emerges[9,10].

A hallmark of cancer is the altered energy metabolism, often characterized by a preference for glycolysis, even in the presence of oxygen, known as the 'Warburg effect'[11]. The Warburg effect signifies increased glycolytic flux and lactate production in cancer cells, aiding cancer progression[12-15]. However, the glucose metabolism in prostatic tissues differs from other tissues. Normal prostate luminal epithelial cells consume substantial amount of glucose to produce citrate for secretion, a specialized function of prostate epithelia[16-19]. At the molecular level, these cells accumulate zinc, inhibiting m-aconitase, an enzyme that converts citrate to isocitrate, thus minimizing citrate oxidation, leading to citrate production and truncated tricarboxylic acid (TCA) cycle in normal prostate[17,20-22]. In transformed PCa cells, however, glucose metabolism undergoes significant changes[23]. Reduced zinc levels enable aconitase to catalyze the conversion of citrate to isocitrate[24-26]. Consequently, citrate accumulation shifts towards citrate oxidation, allowing TCA cycle to proceed[23,27,28]. This alteration results in an increase of TCA cycle flux in PCa cells compared to normal prostate cells[29,30]. Because of this, the Warburg effect is only modest in early-stage PCa[23]. However, advanced AdPCa tumors, similar to many other solid tumors, exhibit more pronounced Warburg effect, which maintains high levels of glycolytic intermediates to support the biosynthesis required for rapid proliferation of the malignant cells[31-33]. As to the glucose metabolism in NEPCa, it remains largely unknown[32].

A key enzyme that regulates glucose metabolism in cancer cells is pyruvate kinase muscle isozyme (PKM)[34-36]. PKM catalyzes the conversion of phosphoenolpyruvate (PEP) to pyruvate, one of the three irreversible and heavily regulated steps in glycolysis[35,37]. PKM has PKM1 and PKM2 isoforms, resulting from alternative splicing[38]. PKM1 incudes exon 9 but not exon 10,

whereas PKM2 includes exon 10 but not exon 9[39]. PKM1 is predominantly expressed in energy-consuming tissues, such as heart, muscle, and brain, where it forms a constitutively active tetramer to promote oxidative phosphorylation[40,41]. In contrast, PKM2 expression is more prevalent in embryonic tissues and cancer cells[42-44]. Unlike PKM1, PKM2 can exist as a catalytically active tetramer or a less active dimer/monomer[45-47]. Its stoichiometry is regulated by allosteric factors and post-translational modifications[47,48]. PKM2 is highly expressed in various cancer types, including AdPCa, contributing to increased glycolytic flux and tumorigenesis in cancer cells[41,43,48-51]. Additionally, in cancer cells, PKM2 is predominantly expressed as dimer, which has lower pyruvate kinase activity, leading to the accumulation of glycolysis intermediates[39,41,42,44]. Apart from PKM1 and PKM2, pyruvate kinase has another two isoforms, PKL and PKR, encoded by PKLR gene, with different promoters[52,53]. PKL is mainly expressed in kidney, liver, and intestine, while PKR is expressed predominantly in red blood cells[53].
A recent study found that in prostate, PKM1 is mostly expressed in stromal cells, whereas PKM2 is expressed in both normal epithelia and cancer cells[54]. It has also been shown that the expression level of PKM2 is higher in prostate adenocarcinomas compared to normal human prostatic tissues and even higher in Gleason 8-10 tumors compared to Gleason 6-7 adenocarcinomas[55,56]. However, the expression of PKM1 and PKM2 in NEPCa, the most aggressive type of prostate cancer, had not been well studied. In this study, using immunohistochemistry (IHC) and immunofluorescence (IF) staining, we assessed the expression of PKM1 and PKM2 during murine prostate development, in PCa mouse models and human prostatic specimens including benign human prostate (BPH), prostate adenocarcinoma (AdPCa), and neuroendocrine prostate cancer (NEPCa).

2. Materials and Methods

2.1 Sample collection

De-identified human prostate tissue specimens were obtained from LSU Health-Shreveport Biorepository Core, Overton Brooks VA Medical Center, Ochsner Health System Biorepository and Tissue for Research organization in accordance with LSU Health-Shreveport IRB protocols. Cell-derived xenograft tumors and murine prostatic tissues derived from wild type mice and tumors of TRAMP mice were from our archival collection.

2.2 Immunohistochemistry and immunofluorescence staining

IHC staining was performed using Vectastain elite ABC peroxidase kit (Vector Laboratories, Burlingame, CA) as described previously[4]. Primary antibodies include PKM1 and PKM2 (7067S, dilution 1:500, and 4053S, dilution 1:1000, respectively, Cell Signaling Technology, Danvers, MA), p63 and FOXA2 (ab735 and ab108422, respectively, dilution 1:500, Abcam, Cambridge, MA), HOXB13 and chromogranin A (CHGA) (sc-28333 and sc-1488, respectively, dilution 1:200, Santa Cruz Biotechnology, Dallas, TX), FOXA1 (A15278, dilution 1:500, Abclonal, Woburn, MA), Synaptophysin (SYP) (611880, dilution 1:1000, BD biosciences, San Jose, CA), and NKX3.1 (0314, dilution 1:500, Athena Enzyme Systems, Baltimore, MD). Images were taken using a Zeiss microscope (White Plains, NY). The intensity of expression was graded as 0 (negative), 1+ (low), 2+ (moderate), and 3+ (high). For IF staining, primary antibodies include CHGA (AB_1553436, dilution 1:50, Developmental Studies Hybridoma Bank, Iowa City, IA), PKM1, PKM2, p63, and SYP (source was the same as mentioned above, dilution 1:100). The IF staining was imaged with a Nikon fluorescence microscope (Melville, NY) as reported previously[57].

2.3 Cell culture

PCa cells VCap, LNCaP, C4-2B, 22RV1, PC3, and DU145 were cultured in RPMI 1640 supplemented with 10% FBS, and 1% penicillin-streptomycin. H660 cells were cultured in Prostalife media (LifeLine Cell Technology, Oceanside, CA). C2C12 cells were cultured in DMEM supplemented with 10% FBS, and 1% penicillin-streptomycin. The differentiation of C2C12 cells were induced by culturing them in DMEM supplemented with 2% horse serum for seven days. Cells were maintained in an incubator at 37 °C with a 5% CO2 atmosphere.

2.4 Western blot

Cells were lysed in Laemmli SDS sample buffer followed by SDS-PAGE and Western blotting. Primary antibodies are beta-actin (sc-47778, dilution 1:500, Santa Cruz Biotechnology, Dallas, TX), PKM1 and PKM2 (the same source as mentioned above, dilution 1:1000), and HRP-conjugated secondary antibody (Cell Signaling, Beverly, MA). Protein bands were visualized by using ProSignal® Dura ECL Reagent (Genesee Scientific, San Diego, CA) and Chemidoc™ Touch Imaging System (Bio-Rad).

2.5 Cross-linking reaction

Cells were washed with ice-cold PBS three times and treated with 1-5mM disuccinimidyl suberate (DSS, A39267, Thermo Scientific, Waltham, MA) for 30 min at room temperature. The

reaction was stopped by adding the quenching solution (1M Tris, PH 7.5) to the final concentration of 20mM for 15 min. Then, cell lysates were used for WB as described above.

2.6 Bioinformatics analysis

RNAseq data in the CTPC collection were analyzed to assess the expression of PKM isoforms using STAR-Salmon based transcript level quantification method[58-61]. The raw Fastq files were downloaded from NCBI SRA database. NCBI human GRCh38 (release 106) and associated GFT files were acquired through "AWS iGenomes" (https://ewels.github.io/AWS-iGenomes/) and were used for alignment. FastQC (https://github.com/s-andrews/FastQC), Trim Galore (https://github.com/FelixKrueger/TrimGalore), STAR[58], Salmon[59] softwares were used for sequencing quality control, alignment and quantification in the Linux Ubuntu environment. The transcript expression was visualized in R (V 4.3.0) environment. The TPM values were first log2 transformed and quantile normalized using "preprocessCore" R package[62]. The data was visualized by boxplot using "ggplot2" R package[63].

3. Results

3.1. The expression of PKM1 and PKM2 in murine prostate

We first examined the expression of PKM1 and PKM2 during murine prostate development, including embryonic prostate undergoing budding morphogenesis (urogenital sinus, UGS), postnatal 2- and 3- week developing prostate, and fully developed 8- week prostate. The prostatic buds in UGS were highlighted by the expression of Foxa2 & p63 and the epithelial cells in postnatal prostate were highlighted by the expression of Hoxb13, Foxa1, and Nkx3.1. We found that PKM1 expression was essentially absent in the developing prostate (Figs. 1A, 1E & 1I) but present in the developed prostate, albeit at low level (Fig. 1M). Moreover, PKM1 was predominantly expressed in the stroma cells of developed prostate (Fig. 2A). In contrast, PKM2 was predominantly expressed in prostatic epithelial cells throughout prostate development (Figs. 1B, 1F, 1J & 1N).

Further, we assessed the expression of PKM1 and PKM2 during murine PCa progression using the transgenic adenocarcinoma of the mouse prostate (TRAMP), a widely used PCa mouse model[64]. TRAMP mice develop prostatic intraepithelial neoplasia (PIN) and a subset of tumors progress into NEPCa[65]. We found that PKM1 expression was present in the epithelial cells of wild-type prostates (Fig. 2A) as well as normal adjacent cells of TRAMP tumors (Fig. 2B) but absent in the PIN lesions of TRAMP mice (Fig. 2B). In the TRAMP tumors that have progressed

to NEPCa, PKM1 was expressed in the NEPCa areas, while its expression remained absent in the PIN lesions (Fig. 2C). In contrast, high PKM2 expression was detected in both the PIN lesions and NEPCa cells of TRAMP tumors (Figs. 2H & 2I). It is noteworthy that the expression level of PKM2 was higher in PIN lesions than the adjacent NEPCa areas in TRAMP tumors (Fig. 2I). To confirm the differential expression of PKM1 and PKM2 in TRAMP tumors, we performed dual immunofluorescence staining of PKMs with NEPCa marker Synaptophysin. PKM1 expression was detected in the NEPCa cells (highlighted by Syp positivity) but not in the adjacent PIN lesion (Figs. 2D-2F). In contrast, PKM2 expression was more prominent in the PIN lesions than the adjacent NEPCa areas (Figs. 2J-2L).

3.2. PKM1 expression is absent in most AdPCa but present in a subset of NEPCa, while PKM2 expression is abundant in most human prostatic tissues.

We also conducted immunohistochemical staining to assess the expression of PKM1 and PKM2 in human prostatic tissues, including benign prostatic hyperplasia (BPH), low-grade and high-grade AdPCa, as well as NEPCa. Consistent with PKMs' expression pattern in murine prostate, PKM1 was predominantly expressed in stroma cells (Fig. 3). In BPH, moderate PKM1 expression was detected in basal epithelial cells (Fig. 3A, n=13). This expression pattern was confirmed by dual immunofluorescence staining of PKM1 with p63, a marker of prostate basal epithelia. The result showed a high expression of PKM1 in stroma cells, with detectable expression in basal epithelial cells as well (Figs. 3E-H). In low-grade and high-grade human prostate adenocarcinoma (AdPCa) samples, PKM1 expression was generally scarce (Figs. 3B & 3C, n=12 and 14, respectively). However, in the high-grade AdPCa cases with NE differentiation, PKM1 was expressed in the rare NE cells, which were highlighted by the co-expression of NEPCa marker CHGA (Figs. 3I-L). Additionally, PKM1 expression was detected in 5/12 human NEPCa samples (Fig. 3D). The PKM1 expression in PCa cells, including both AdPCa and NEPCa, was quantified and its distribution among PCa samples was presented in Fig. 3Q.

Moreover, we examined the expression of PKM1 in other types of NE tumors, including pancreatic adenocarcinoma with NE differentiation (Fig. 3M, 4/4 positive), Merkel cell carcinoma (Fig. 3N, 2/3 positive), SCLC (Fig. 3O, 1/2 positive), urothelial NE carcinoma (Fig. 3P, 2/3 positive). We found that PKM1 was expressed in a subset of these NE tumors as well, highlighting its potential role in the pathogenesis of neuroendocrine cancers.

On the other hand, the expression of PKM2 was detected in the majority of human prostatic tissues. In the BPH samples, PKM2 expression was prominent in basal epithelial cells and comparatively moderate in luminal epithelial cells (Figs. 4A & 4B, n=14). This expression pattern was confirmed by dual immunofluorescence staining, which indicated PKM2 was highly expressed in basal epithelial cells (highlighted by basal marker p63), with less staining in luminal epithelial cells (Figs. 4I-L). Human AdPCa samples exhibited a diverse PKM2 expression pattern, varying from negative to high in low-grade AdPCa (Figs. 4C& 4D, n=12) and high-grade AdPCa (Figs. 4E & 4F, n=15). Additionally, PKM2 was expressed in all the human NEPCa samples examined (Figs. 4G & 4H, n=9). The intensity of PKM2 staining in PCa cells, including both AdPCa and NEPCa, was quantified and its distribution among PCa samples was presented in Fig. 4M.

Taken together, PKM2 was predominantly expressed in human prostatic tissues, ranging from benign to cancerous prostate, including both AdPCa and NEPCa. PKM1 expression in PCa was limited but notable, showing low to moderate expression in a subset of NEPCa cases.

3.3. The expression of PKM1 and PKM2 in human PCa cell lines.

We evaluated the expression of PKM1 and PKM2 in PCa cell lines, including AR positive (VCaP, LNCaP, C42B and 22RV1), AR negative (PC3 and DU145), and NEPCa (H660) cell lines. Both cultured cells and cell-derived xenograft tumors were used. Immunohistochemical staining indicated the expression of PKM1 was lowest in 22RV1- and highest in PC3- derived xenograft tumors (Figs. 5A-G). This expression pattern was consistent with the Western blot analysis of the lysates derived from in vitro-cultured cells (Fig. 5H). NEPCa H660 cells expressed moderate level of PKM1 (Fig. 5H). PKM2 expression was consistently detected in all seven cell lines (Figs. 5I-P).

3.4 Bioinformatic analysis revealed the expression of PKM1/2 transcripts in PCa cell lines and patient samples

As the splicing isoforms of PKM, the PKM1/2 transcripts are classified based on the difference in a single exon resulted from an exclusive exon 9 or 10 skipping. PKM1 isoforms retain exon 9 and PKM2 isoforms retain exon 10. Antibodies were generated to distinctively target exon 9 or exon 10, but these antibodies cannot differentiate the various isoforms of each PKM class. The development of high through-put RNA sequencing and associated bioinformatic tools enables analyzing each of these isoforms. Using the publicly available RNAseq data generated from

human PCa cell lines and patient samples, we identified and quantified the transcripts of 10 PKM isoforms including the previously well-studied PKM1 isoforms (NM_182470.2 and NM_182471.2) and PKM2 isoform (NM_002654.4) as well as other under studied isoforms. The ten PKM isoforms were presented in Fig. 6A, and the expression levels of each isoform in human prostatic tissue specimens were summarized in Fig. S2. Based on the inclusion of exon 9 or exon 10, these isoforms were classified into "PKM1-like" and "PKM2-like" transcripts, respectively. The antibodies that target exon 9 or 10, in fact, detect the protein products of PKM1-like or PKM2-like transcripts. The PKM1-like transcripts consisted of 4 isoforms, among which NM_182470.2 and NM_182471.2 transcripts encode the same protein since the only difference in them lies within their 5 UTRs. The protein encoded by these two isoforms was previously known as PKM1. There are six PKM2-like isoforms, among which NM_002654.4 transcript encodes a protein that was previously known as PKM2.

To complement our bioinformatics analysis with previous protein expression data, we summed the normalized log2-transformed TPM values of NM_182470.2 and NM_182471.2 as PKM1 transcript. The expression data of NM_002654.4 were directly used to reflect the levels of PKM2 transcript. Additionally, to coordinate our bioinformatics analysis with PKM1/2 antibodies' staining results, we summed the values of all exon 9-retained transcripts as PKM1-like expression data and all exon 10-retained transcripts as PKM2-like expression data. Overall, the levels of PKM2-like transcripts were higher than that of PKM1-like transcripts in both PCa cell lines and human PCa specimens (Figs. 6B & 6C). The NM_002654.4 transcript was the dominant PKM2 isoform expressed in these tissues (Fig. S1).

Additionally, we analyzed the prostatic expression of PKL/R, the other two PK isoforms[61]. We found the levels of PKL/R transcripts were generally not high in human PCa cell lines or human PCa except a subset of human PCa specimens including NEPCa (Fig. S2).

3.5 The stoichiometry of PKM2.

PKM1 is constitutively active as a tetramer[39]. PKM2 can exist as a monomer, dimer, or tetramer which is regulated by its allosteric regulator, like serine, and FBP, as well as post-translational modifications, like phosphorylation and oxidation[45-47]. In many cancer types, PKM2 predominantly forms a monomer/dimer, which exhibits low pyruvate kinase activity, leading to the accumulation of glycolysis intermediates and the production of lactate in cancer cells[39,41,42]. To elucidate the role of PKM2 in PCa, we conducted the cross-linking reaction using human PCa

cell lines. C2C12 was used as a positive control for the cross-linking reaction (Fig. 7A). C2C12 is a myoblast cells expressing high PKM2, can be differentiated into myotubes which exhibit high PKM1 expression level[66]. We detected the monomer and dimer but not tetramer formation of PKM2 in PCa cell lines (Fig. 7B), indicating that PKM2, the predominant isoform of PKM in PCa cells, exists in the stoichiometry of low pyruvate kinase activity.

4. Discussion

There is a paucity of NEPCa specimens because surgery is not the primary treatment for late-stage PCa patients and these patients are not usually biopsied. This has limited research on the energy metabolism of NEPCa. In this study, using the human prostatic samples we have collected as well as archived murine PCa tissues, we assessed the expression of PKM isoforms during prostate development and PCa progression including both AdPCa and NEPCa. We found that PKM2 was the predominant form expressed in prostatic tissues and PKM1 expression is less prominent in prostate epithelia or AdPCa cells. Consistent with previous reports[54,67], PKM1 was highly expressed in the stromal cells in both benign and cancerous prostatic tissues. Prostatic basal epithelial cells expressed ample PKM1 as well, suggesting these cells may have distinct glucose metabolism. Basal cells are absent in PCa, and PKM1 expression is restricted to the stroma regions in the tumors. This expression pattern suggests PKM1 may play an insignificant role in AdPCa. In contrast, PKM2 is expressed in prostate epithelial cells. Its level is generally higher in high-grade AdPCa compared with normal prostate or low-grade AdPCa. Given the well-established function of PKM2 in regulating glucose metabolism, elevated PKM2 in high-grade AdPCa aligns well with the increased Warburg effect in these tumors. This notion is further supported by previous studies that have shown PKM2 knockdown reduces lactate production and inhibits cell proliferation in DU145 cells, and Pkm2 knockout suppresses tumor progression in Pten null mice[54,56]. Taken together, these studies indicate that PKM2 promotes Warburg effects and carcinogenesis of AdPCa.

PKM1 and PKM1-like transcripts are detected in normal human prostate samples. This is likely attributed to the high PKM1 expression in stromal cells. Importantly, PKM1 is co-expressed with NEPCa markers in human PCa tissues that have NE differentiation, but its expression is absent in the adjacent non-NEPCa cells. Additionally, PKM1 is expressed in a subset of NEPCa tumors. Albeit low, its expression level is still higher in NEPCa than PIN and AdPCa. Moreover, we found PKM1 is expressed in other types of NE tumors as well including small cell lung cancer.

This is consistent with literatures that report PKM1 expression in pulmonary NE tumors[68]. In contrast, PKM2 is highly expressed in all prostatic tissues but its level is notably lower in NEPCa than AdPCa.

Using publicly available RNAseq data, we analyzed the expression of ten PKM isoforms in prostatic tissues. These isoforms were categorized into PKM1- and PKM2- like groups, based on the presence of exon 9 and exon 10, respectively. We found that PKM2 was the most prominent isoform expressed in prostatic tissues, at a level much higher than all the other nine isoforms, suggesting its dominant role in prostatic tissues, except in PC3 cells where both PKM1 and PKM2 are highly expressed. It would be interesting to study the functional involvement of PKM1 and PKM2 in this cell line.

The antibodies that specifically target exon 9 or 10 can differentiate the PKM1-like from PKM2-like groups but not the individual isoforms. It is worthy to note that the ten PKM isoforms encode proteins of different molecular weight, which may enable the detection of certain isoforms within the PKM1-like and PKM2-like groups by Western blotting. However, our Western blot result only displayed single PKM band. Coupled with the dominant transcript count data, we suggest that the prevalent protein isoforms in PCa are PKM1 encoded by NM_182470.2 & NM_182471.2 and PKM2 encoded by NM_002654.4 transcripts.

In addition to PKM1 and PKM2, we identified seven other PKM isoforms. Although their expression level is not high in prostatic tissues, it may still be worthy to take into consideration of their existence when studying pyruvate kinases in PCa. Indeed, s recent study indicates that PKLR expression is increased in castrate-resistant PCa and the upregulated PKLR/MYCN pathway may drive the metabolic reprogramming during NE differentiation[69].

Taken together, our study characterized the expression of PKM1 and PKM2 in prostatic tissues including developing, benign, and cancerous prostate. This information contributes to our better understanding of the metabolic alterations in aggressive PCa and may potentially lead to the development of targeted therapies to combat this deadly disease. However, due to the scarcity of NEPCa specimens, further research is warranted to fully comprehend the metabolic profile of this aggressive PCa subtype and explore potential therapeutic avenues.

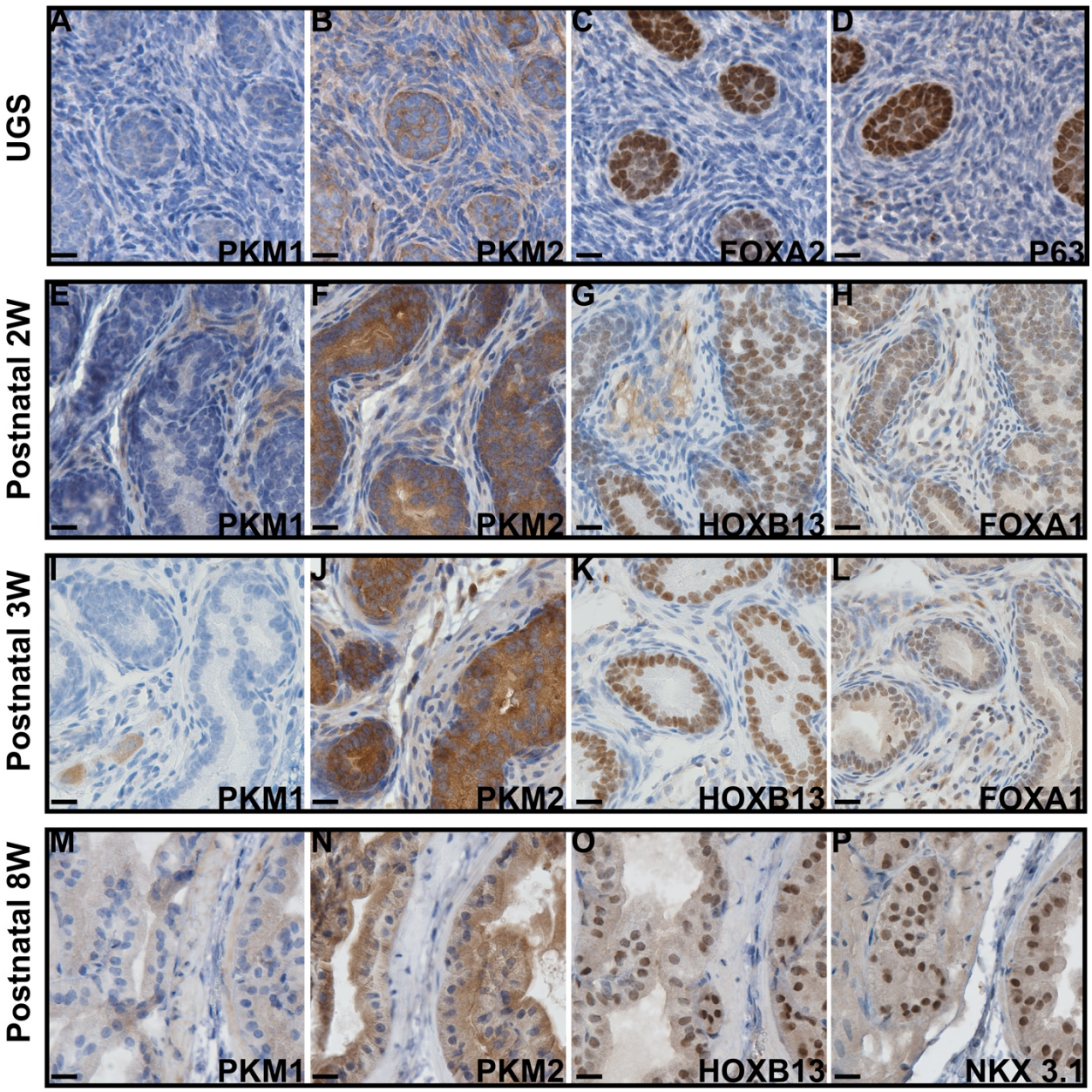

Figure 1. The expression of PKM1 and PKM2 in mice prostate. (A-P) IHC staining of PKM1 (**A**, **E**, **I**, and **M**), PKM2 (**B**, **F**, **J**, and **N**), prostatic markers FOXA2 (**C**), basal epithelial marker p63 (**D**), HOXB13 (**G**, **K**, and **O**), FOXA1 (**H**, and **L**) and NKX3.1 (**O**) in mice urogenital sinus (UGS), and mice prostate at 2 weeks (2W), 3 weeks (3W), and 8 weeks (8W) postnatal. Scale bar = 20 μM.

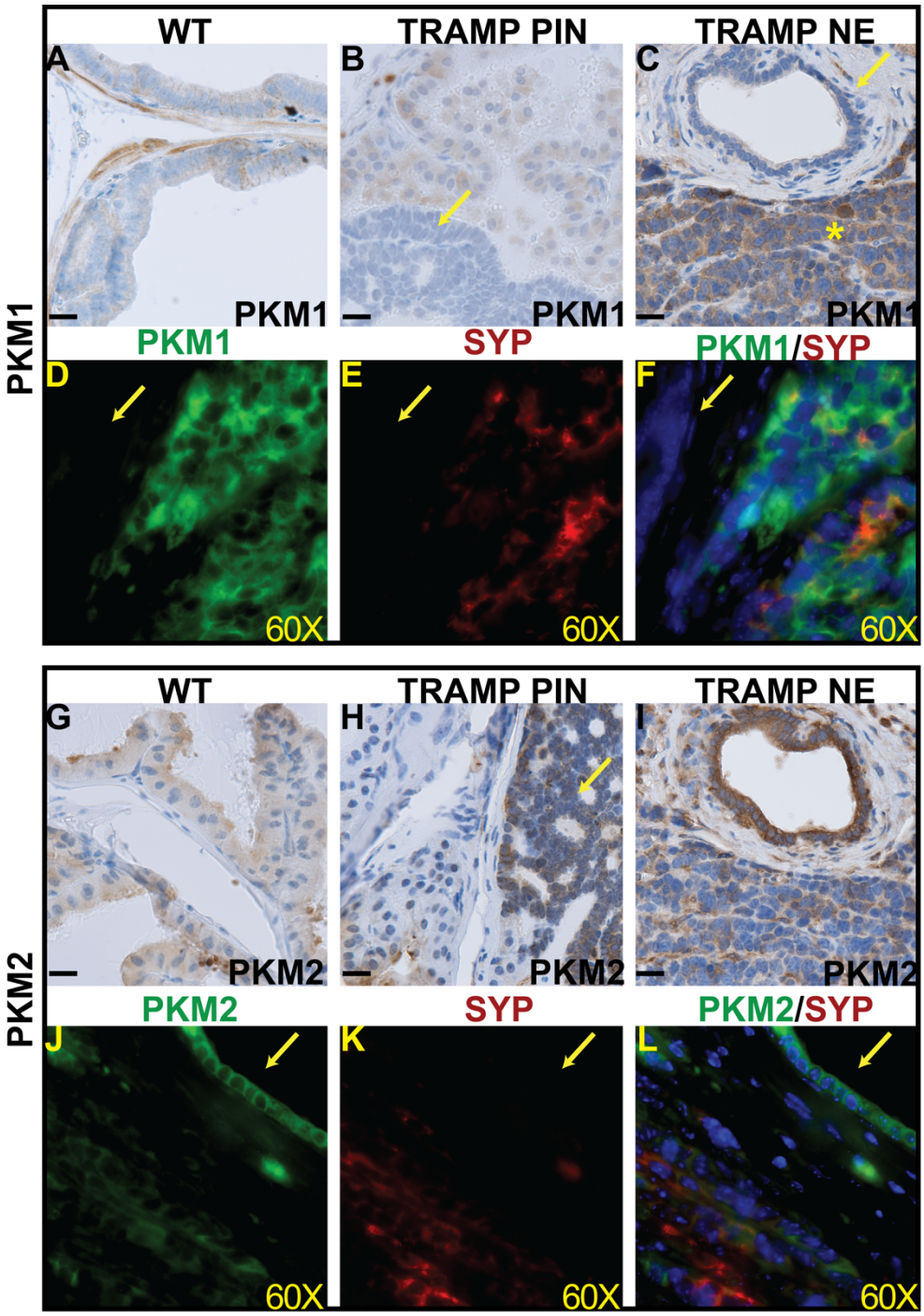

Figure 2. The expression of PKM1 and PKM2 in murine prostate. (**A-C**) IHC staining of PKM1 in wild-type (**A**), TRAMP PIN (**B**) and TRAMP NE (**C**). (**D-F**) Dual IF staining of PKM1 (**D**, green) with NE marker SYP (**E**, red)) in TRAMP mice. (**G-I**) IHC staining of PKM2 in wild-type (**G**), TRAMP PIN (**H**) and TRAMP NE (**I**). (**J-L**) Dual IF staining of PKM1 (**J**, green) with NE marker SYP (**K**, red)) in TRAMP mice. The yellow arrows denote prostatic intraepithelial neoplasia (PIN) lesions. Astrids denote NEPCa. IHC Scale bar = 20 μM. IF were taken using 60X lens.

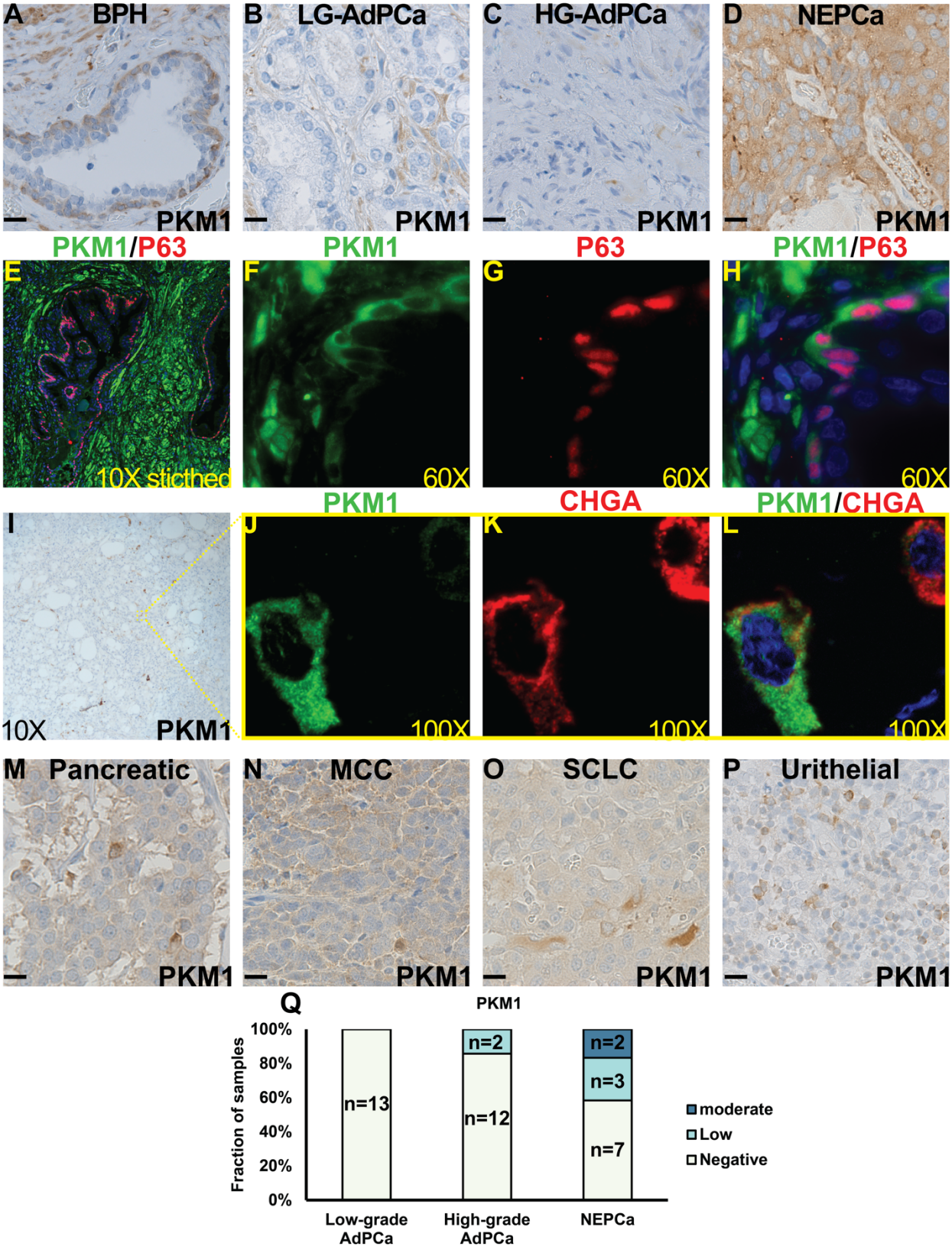
A BPH
PKM1
B LG-AdPCa
PKM1
C HG-AdPCa
PKM1
D NEPCa
PKM1
PKM1/P63
E
10X stictheo
PKM1
F
60X
P63
G
60X
PKM1/P63
H
60X
I
10X
PKM1
PKM1
J
100X
CHGA
K
100X
PKM1/CHGA
L
100X
M Pancreatic
PKM1
N MCC
PKM1
O SCLC
PKM1
P Urithelial
PKM1
Q
PKM1
Fraction of samples
100%
80%
60%
40%
20%
0%
n=13
n=2
n=12
n=2
n=3
n=7
moderate
Low
Negative
Low-grade AdPCa
High-grade AdPCa
NEPCa

Figure 3. The expression of PKM1 in human prostate specimens and other NE tumors. (**A-D**) IHC staining of PKM1 in BPH (**A**), low-grade (LG) AdPCa (**B**), high-grade (HG) AdPCa **(C)** and NEPCa **(D**). The quantification of PKM1 IHC staining intensity in human PCa was shown in (**Q**). (**E-H**) IF staining of PKM1 (**F**, green) and basal epithelial cell marker p63 (**G**, red) in human BPH. (**I-L**) serial sections derived from an AdPCa with NED were stained with PKM1 (**I**, IHC), or co-stained (IF, PKM1, **J**, green) with NE marker CHGA (**K**, red). (**M-P**) IHC staining of PKM1 in pancreatic adenocarcinoma with NED sample (**M**, n=4), Merkel cell carcinoma (MCC) sample (**N**, n=3), small cell lung cancer (SCLC) sample (**O**, n=2), and urothelial NED samples (**P**, n=3). Scale bar for IHC = 20 μM.

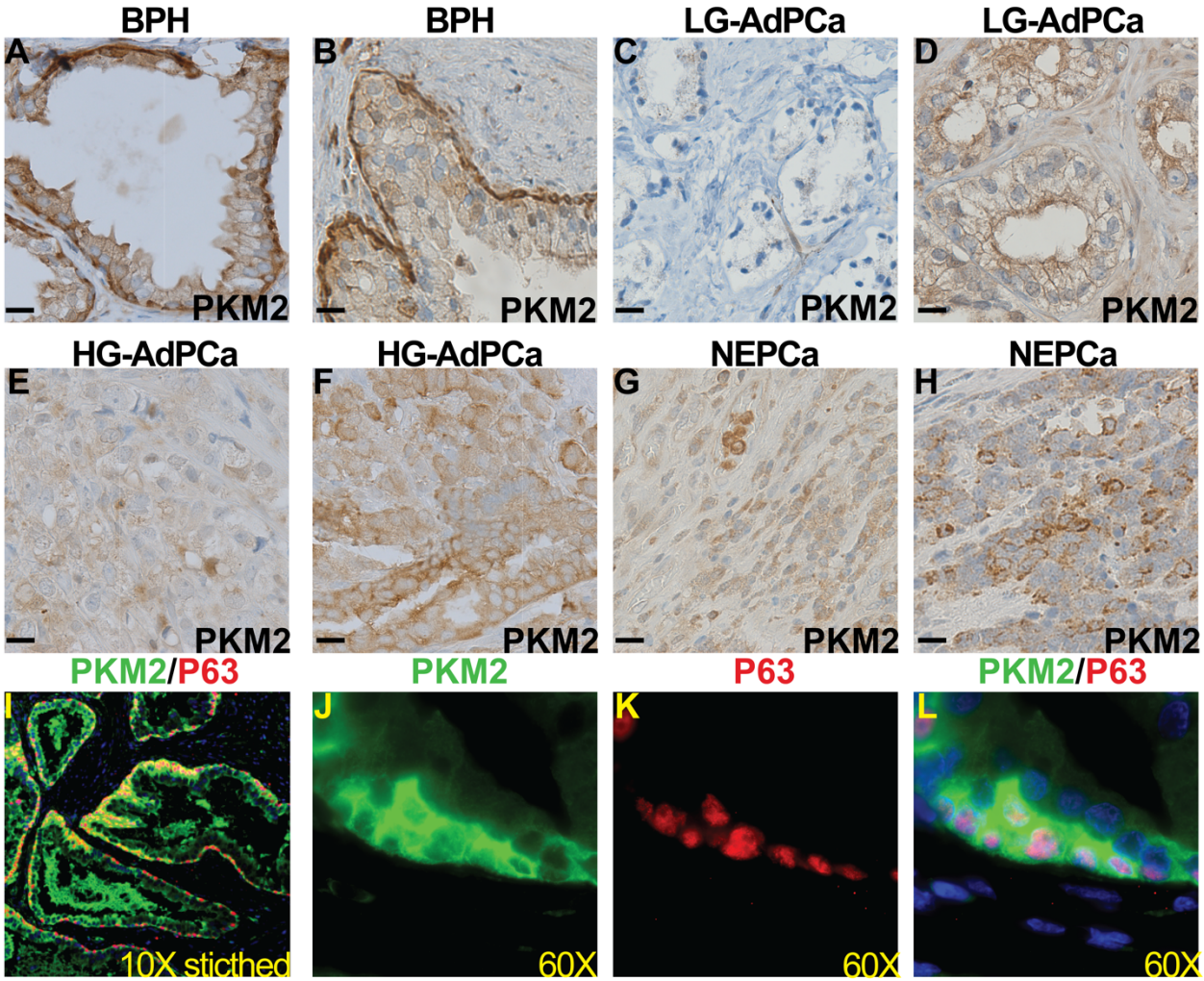
BPH
A
PKM2
BPH
B
PKM2
LG-AdPCa
C
PKM2
LG-AdPCa
D
PKM2
HG-AdPCa
E
PKM2
HG-AdPCa
F
PKM2
NEPCa
G
PKM2
NEPCa
H
PKM2
PKM2/P63
I
10X sticthed
PKM2
J
60X
P63
K
60X
PKM2/P63
L
60X

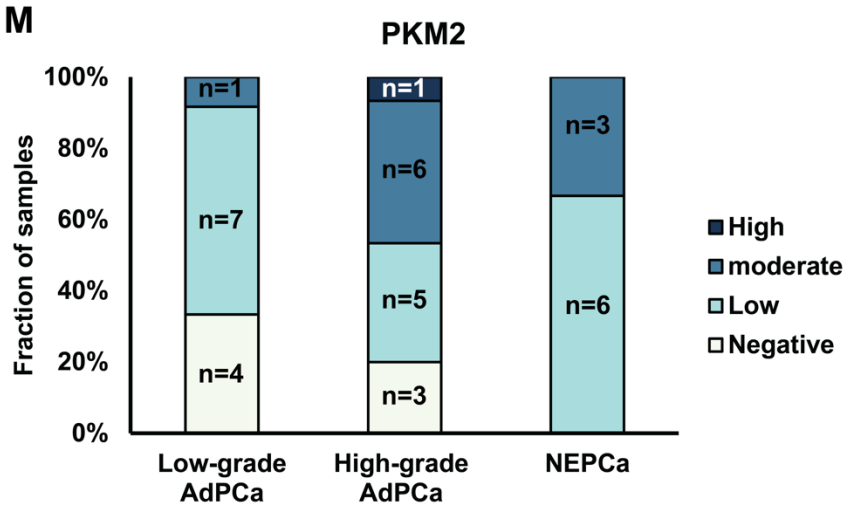
M
PKM2
Fraction of samples
100%
80%
60%
40%
20%
0%
n=1
n=7
n=4
n=1
n=6
n=5
n=3
n=3
n=6
Low-grade AdPCa
High-grade AdPCa
NEPCa
High
moderate
Low
Negative

Figure 4. The expression of PKM2 in human prostate specimens. (A-H) IHC staining of PKM2 in BPH (**A** & **B**), low-grade (LG) AdPCa (**C** & **D**), high-grade (HG) AdPCa (**E** & **F**) and NEPCa (**G** & **H**) samples. **(I-L)** IF staining of PKM2 (**B**, green) and basal epithelial cell marker p63 (**C**, red) in human BPH. (**M**) represented the quantification of PKM2 staining intensity. Scale bar for IHC = 20 μM.

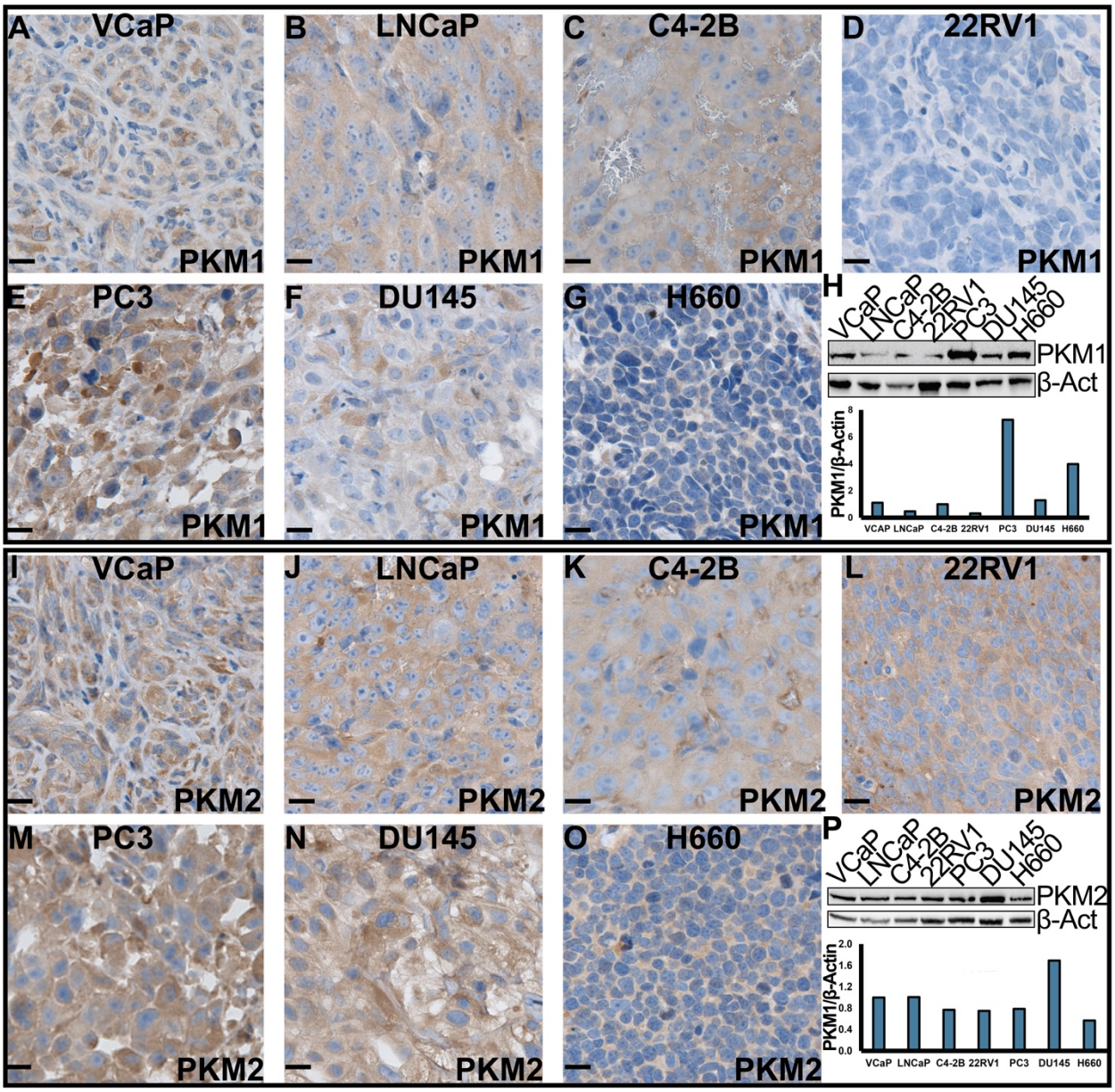

Figure 5. The expression of PKM1 and PKM2 in human PCa cell lines. (**A-G,** and **I-O**) IHC staining of PKM1 and PKM2, respectively, in xenograft tumors derived from PCa cell lines. Scale bar = 20 μM. (**H** & **P**) Western blotting and quantification for protein levels of PKM1 (**H**) and PKM2 (**P**), respectively, in human PCa cell lines.

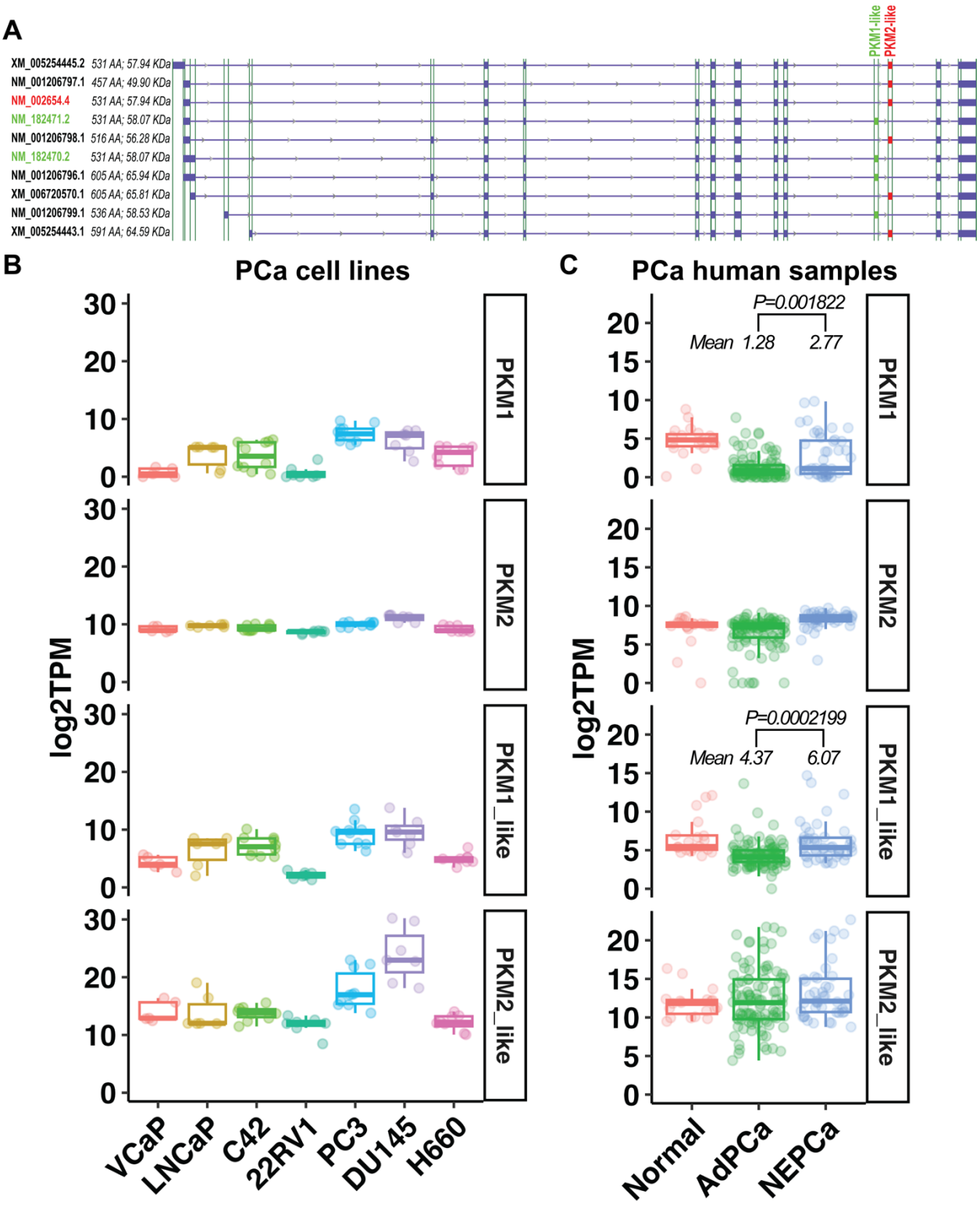
A
PKM1-like
PKM2-like
XM_005254445.2 531 AA; 57.94 KDa
NM_001206797.1 457 AA; 49.90 KDa
NM_002654.4 531 AA; 57.94 KDa
NM_182471.2 531 AA; 58.07 KDa
NM_001206798.1 516 AA; 56.28 KDa
NM_182470.2 531 AA; 58.07 KDa
NM_001206796.1 605 AA; 65.94 KDa
XM_006720570.1 605 AA; 65.81 KDa
NM_001206799.1 536 AA; 58.53 KDa
XM_005254443.1 591 AA; 64.59 KDa
B
PCa cell lines
log2TPM
PKM1
PKM2
PKM1_like
PKM2_like
VCaP
LNCaP
C42
22RV1
PC3
DU145
H660
C
PCa human samples
P=0.001822
Mean 1.28
2.77
P=0.0002199
Mean 4.37
6.07
Normal
AdPCa
NEPCa

Figure 6. The expression of PKM1-like and PKM2-like isoforms in human PCa. (A) Ten identified PKM isoforms transcripts and molecular weight. Green labeled two PKM1 and PKM1-like isoforms with expression of exon 9. Red labeled PKM2 and PKM2-like isoforms with expression of exon 10. (**B** & **C**) The mRNA expression of PKM1, PKM2, PKM1-like, and PKM2-like in human PCa cell line and human patients samples. Each dot in the plot represents the gene expression level of one study.

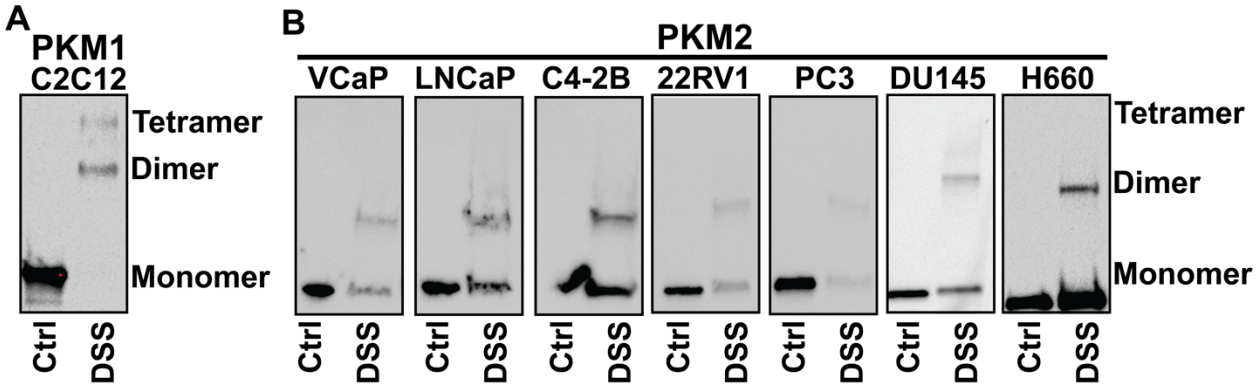

Figure 7. The stoichiometry of PKMs. Cells were treated with DSS reagent to form intramolecular crosslinks and Western blot analysis was conducted to detect the PKM1 and PKM2 subunit association in Pca cells. (**A**) Differentiated myoblast C2C12 cells were used as a positive control for DSS cross-linking reaction. (**B**) PCa cells did not express detectable tetramer forms of PKM2.

References

1 McNeal, J. E. Normal histology of the prostate. *The American journal of surgical pathology* **12**, 619-633 (1988).

2 Dehm, S. M. & Tindall, D. J. Molecular regulation of androgen action in prostate cancer. *Journal of cellular biochemistry* **99**, 333-344 (2006).

3 Robinson, D. *et al.* Integrative clinical genomics of advanced prostate cancer. *Cell* **161**, 1215-1228 (2015).

4 Cheng, S. *et al.* Neuroendocrine prostate cancer has distinctive, non-prostatic HOX code that is represented by the loss of HOXB13 expression. *Scientific reports* **11**, 1-11 (2021).

5 Litwin, M. S. & Tan, H.-J. The diagnosis and treatment of prostate cancer: a review. *Jama* **317**, 2532-2542 (2017).

6 Chandrasekar, T., Yang, J. C., Gao, A. C. & Evans, C. P. Mechanisms of resistance in castration-resistant prostate cancer (CRPC). *Translational andrology and urology* **4**, 365 (2015).

7 Fujita, K. & Nonomura, N. Role of androgen receptor in prostate cancer: a review. *The world journal of men's health* **37**, 288-295 (2019).

8 Rubin, M. A., Bristow, R. G., Thienger, P. D., Dive, C. & Imielinski, M. Impact of lineage plasticity to and from a neuroendocrine phenotype on progression and response in prostate and lung cancers. *Molecular cell* **80**, 562-577 (2020).

9 Beltran, H. *et al.* Divergent clonal evolution of castration-resistant neuroendocrine prostate cancer. *Nature medicine* **22**, 298-305 (2016).

10 Ferguson, A. M. & Rubin, M. A. Lineage plasticity in prostate cancer: Looking beyond intrinsic alterations. *Cancer Letters*, 215901 (2022).

11 Hanahan, D. & Weinberg, R. A. Hallmarks of cancer: the next generation. *cell* **144**, 646-674 (2011).

12 Kim, J.-w. & Dang, C. V. Cancer's molecular sweet tooth and the Warburg effect. *Cancer research* **66**, 8927-8930 (2006).

13 Vander Heiden, M. G., Cantley, L. C. & Thompson, C. B. Understanding the Warburg effect: the metabolic requirements of cell proliferation. *science* **324**, 1029-1033 (2009).

14 Liberti, M. V. & Locasale, J. W. The Warburg effect: how does it benefit cancer cells? *Trends in biochemical sciences* **41**, 211-218 (2016).

15 DeBerardinis, R. J. & Chandel, N. S. We need to talk about the Warburg effect. *Nature metabolism* **2**, 127-129 (2020).

16 Cooper, J. F. & Farid, I. The role of citric acid in the physiology of the prostate: III. lactate/citrate ratios in benign and malignant prostatic homogenates as an index of prostatic malignancy. *The Journal of urology* **92**, 533-536 (1964).

17 Costello, L. C. & Franklin, R. B. Aconitase activity, citrate oxidation, and zinc inhibition in rat ventral prostate. *Enzymologia biologica et clinica* **26**, 281-287 (1981).

18 Costello, L. C. & Franklin, R. B. Concepts of citrate production and secretion by prostate 1. Metabolic relationships. *The Prostate* **18**, 25-46 (1991).

19 Costello, L. C. & Franklin, R. B. A comprehensive review of the role of zinc in normal prostate function and metabolism; and its implications in prostate cancer. *Archives of biochemistry and biophysics* **611**, 100-112 (2016).

20 Costello, L. C., Liu, Y., Franklin, R. B. & Kennedy, M. C. Zinc inhibition of mitochondrial aconitase and its importance in citrate metabolism of prostate epithelial cells. *Journal of Biological Chemistry* **272**, 28875-28881 (1997).

21 Costello, L. C., Franklin, R. B. & Feng, P. Mitochondrial function, zinc, and intermediary metabolism relationships in normal prostate and prostate cancer. *Mitochondrion* **5**, 143-153 (2005).

22 Franklin, R. B., Milon, B., Feng, P. & Costello, L. C. Zinc and zinc transporters in normal prostate function and the pathogenesis of prostate cancer. *Frontiers in bioscience: a journal and virtual library* **10**, 2230 (2005).

23 Lin, C. *et al.* Prostate cancer energetics and biosynthesis. *Prostate Cancer*, 185-237 (2019).

24 Franklin, R. B. *et al.* hZIP1 zinc uptake transporter down regulation and zinc depletion in prostate cancer. *Molecular cancer* **4**, 1-13 (2005).

25 Desouki, M. M., Geradts, J., Milon, B., Franklin, R. B. & Costello, L. C. hZip2 and hZip3 zinc transporters are down regulated in human prostate adenocarcinomatous glands. *Molecular cancer* **6**, 1-7 (2007).

26 Costello, L. C. & Franklin, R. B. Zinc is decreased in prostate cancer: an established relationship of prostate cancer! *JBIC Journal of Biological Inorganic Chemistry* **16**, 3-8 (2011).

27 Feng, P. *et al.* Zinc induces mitochondria apoptogenesis in prostate cells. *Molecular urology* **4** (2000).

28 Eidelman, E., Twum-Ampofo, J., Ansari, J. & Siddiqui, M. M. The metabolic phenotype of prostate cancer. *Frontiers in oncology* **7**, 131 (2017).

29 Naruse, K. *et al.* Lactate dehydrogenase is a prognostic indicator for prostate cancer patients with bone metastasis. *泌尿器科紀要* **53**, 287-292 (2007).

30 Elia, I., Schmieder, R., Christen, S. & Fendt, S.-M. Organ-specific cancer metabolism and its potential for therapy. *Metabolic Control*, 321-353 (2016).

31 Wang, J. *et al.* Increased expression of glycolytic enzymes in prostate cancer tissues and association with Gleason scores. *International Journal of Clinical and Experimental Pathology* **10**, 11080 (2017).

32 Ahmad, F., Cherukuri, M. K. & Choyke, P. L. Metabolic reprogramming in prostate cancer. *British journal of cancer* **125**, 1185-1196 (2021).

33 Cardoso, H. J. *et al.* Revisiting prostate cancer metabolism: From metabolites to disease and therapy. *Medicinal Research Reviews* **41**, 1499-1538 (2021).

34 Nelson, D. L., Lehninger, A. L. & Cox, M. M. *Lehninger principles of biochemistry*. (Macmillan, 2008).

35 Li, X. b., Gu, J. d. & Zhou, Q. h. Review of aerobic glycolysis and its key enzymes–new targets for lung cancer therapy. *Thoracic cancer* **6**, 17-24 (2015).

36 Abbaszadeh, Z., Çeşmeli, S. & Avcı, Ç. B. Crucial players in glycolysis: cancer progress. *Gene* **726**, 144158 (2020).

37 Fothergill-Gilmore, L. A. & Michels, P. A. M. Evolution of glycolysis. *Progress in biophysics and molecular biology* **59**, 105-235 (1993).

38 Chen, M., Zhang, J. & Manley, J. L. Turning on a Fuel Switch of Cancer: hnRNP Proteins Regulate Alternative Splicing of Pyruvate Kinase mRNAhnRNP Proteins Regulate PKM Splicing. *Cancer research* **70**, 8977-8980 (2010).

39 Wu, S. & Le, H. Dual roles of PKM2 in cancer metabolism. *Acta Biochim Biophys Sin* **45**, 27-35 (2013).

40 Peterson, J. S., Chern, C. J., Harkins, R. N. & Black, J. A. The subunit structure of human muscle and human erythrocyte pyruvate kinase isozymes. *FEBS letters* **49**, 73-77 (1974).

41 Zahra, K., Dey, T., Mishra, S. P. & Pandey, U. Pyruvate kinase M2 and cancer: the role of PKM2 in promoting tumorigenesis. *Frontiers in oncology* **10**, 505842 (2020).

42 Luo, W. & Semenza, G. L. Emerging roles of PKM2 in cell metabolism and cancer progression. *Trends in Endocrinology & Metabolism* **23**, 560-566 (2012).

43 Yang, W. & Lu, Z. Regulation and function of pyruvate kinase M2 in cancer. *Cancer letters* **339**, 153-158 (2013).

44 Wong, N., Ojo, D., Yan, J. & Tang, D. PKM2 contributes to cancer metabolism. *Cancer letters* **356**, 184-191 (2015).

45 Takenaka, M. *et al.* Isolation and characterization of the human pyruvate kinase M gene. *European journal of biochemistry* **198**, 101-106 (1991).

46 Ashizawa, K., Willingham, M. C., Liang, C. M. & Cheng, S.-Y. In vivo regulation of monomer-tetramer conversion of pyruvate kinase subtype M2 by glucose is mediated via fructose 1, 6-bisphosphate. *Journal of Biological Chemistry* **266**, 16842-16846 (1991).

47 Dombrauckas, J. D., Santarsiero, B. D. & Mesecar, A. D. Structural basis for tumor pyruvate kinase M2 allosteric regulation and catalysis. *Biochemistry* **44**, 9417-9429 (2005).

48 Yang, W. & Lu, Z. Pyruvate kinase M2 at a glance. *Journal of cell science* **128**, 1655-1660 (2015).

49 Iqbal, M. A., Gupta, V., Gopinath, P., Mazurek, S. & Bamezai, R. N. K. Pyruvate kinase M2 and cancer: an updated assessment. *FEBS letters* **588**, 2685-2692 (2014).

50 Dayton, T. L., Jacks, T. & Vander Heiden, M. G. PKM 2, cancer metabolism, and the road ahead. *EMBO reports* **17**, 1721-1730 (2016).

51 Israelsen, W. J. & Vander Heiden, M. G. 43-51 (Elsevier).

52 Zhang, Z. *et al.* PKM2, function and expression and regulation. *Cell & bioscience* **9**, 1-25 (2019).

53 Noguchi, T., Yamada, K., Inoue, H., Matsuda, T. & Tanaka, T. The L-and R-type isozymes of rat pyruvate kinase are produced from a single gene by use of different promoters. *Journal of Biological Chemistry* **262**, 14366-14371 (1987).

54 Davidson, S. M. *et al.* Pyruvate kinase M1 suppresses development and progression of prostate adenocarcinoma. *Cancer research* **82**, 2403-2416 (2022).

55 Wong, N. *et al.* Changes in PKM2 associate with prostate cancer progression. *Cancer investigation* **32**, 330-338 (2014).

56 Dey, P. *et al.* PKM2 Knockdown Induces Autophagic Cell Death via the AKT/mTOR Pathway in Human Prostate Cancer Cells. (2019).

57 Cheng, S. *et al.* The expression of YAP1 is increased in high-grade prostatic adenocarcinoma but is reduced in neuroendocrine prostate cancer. *Prostate cancer and prostatic diseases* **23**, 661-669 (2020).

58 Dobin, A. *et al.* STAR: ultrafast universal RNA-seq aligner. *Bioinformatics* **29**, 15-21 (2013).

59 Patro, R., Duggal, G., Love, M. I., Irizarry, R. A. & Kingsford, C. Salmon provides fast and bias-aware quantification of transcript expression. *Nature methods* **14**, 417-419 (2017).

60 Cheng, S. & Yu, X. CTPC, a combined transcriptome data set of human prostate cancer cell lines. *The Prostate* **83**, 158-161 (2023).

61 Cheng, S., Li, L., Shi, Y. & Yu, X. HuPSA and MoPSA Atlases Revealed Novel Cell Populations and Lineage Plasticity at Single-Cell Resolution in Prostate Cancer. *bioRxiv*, 2023-2008 (2023).

62 Bolstad, B. M. preprocessCore: A collection of pre-processing functions. *R package version* **1**, 2 (2013).

63 Wickham, H. *Data analysis*. (Springer, 2016).

64 Greenberg, N. M. *et al.* Prostate cancer in a transgenic mouse. *Proceedings of the National Academy of Sciences* **92**, 3439-3443 (1995).

65 Huss, W. J. *et al.* Origin of androgen-insensitive poorly differentiated tumors in the transgenic adenocarcinoma of mouse prostate model. *Neoplasia* **9**, 938-IN931 (2007).

66 Clower, C. V. *et al.* The alternative splicing repressors hnRNP A1/A2 and PTB influence pyruvate kinase isoform expression and cell metabolism. *Proceedings of the National Academy of Sciences* **107**, 1894-1899 (2010).

67 Chiavarina, B. *et al.* Pyruvate kinase expression (PKM1 and PKM2) in cancer-associated fibroblasts drives stromal nutrient production and tumor growth. *Cancer biology & therapy* **12**, 1101-1113 (2011).

68 Morita, M. *et al.* PKM1 confers metabolic advantages and promotes cell-autonomous tumor cell growth. *Cancer cell* **33**, 355-367 (2018).